

# LED-photoresistor mechanical-electrical optoisolator transducers

I. M. CIURUȘ\*, M. DIMIAN, A. GRAUR

„Ștefan cel Mare” University, Str. Universitatii nr. 13, Suceava, Romania

LED-photoresistor mechanical-electrical optoisolator transducers are Polaroid optocouplers specialized in converting rotation/translation movements into electrical signals. The processes standing at the basis of such conversion are: light's polarization, re-orientation of the polarizing plan and modification of the distance between source and photoreceiver. This device is at the crossroad of three research directions: MEMS, Smart Lighting and that one of sensors and transducers.

(Received February 1, 2011; accepted August 10, 2011)

*Keywords:* Transducer, Polaroid optocoupler, Polaroid filters, Polarized LED, Photoresistor.

## 1. Introduction

A general view on the evolution of technology from the last 20 years outlines the main directions on which the research in this field will be focused in the future.

One of the interest domains is that one of sensors and transducers.

Sensors and transducers represent the interface between electronic devices and environment.

The new technologies need cheap sensors and transducers, with a low energy consumption, which can convert varied signals into electrical signals. This fact determines the continuous need for their optimization, diversification and miniaturization [1], [2].

The need for sensors and transducers' minimization as well as the need of the devices to which they are connected, have lead to the appearance of the Micro-Electro-Mechanical Systems (MEMS). MEMS is a technology permitting the design of some smart devices with low energy consumption [3], [4].

Another research domain is that one of the "intelligent light". This domain aims at developing sources of intelligent light which can change the way in which society uses light [5], [6].

In this article is presented a device designed by us, which is at the crossroad of three research directions: MEMS, Smart Lighting and that one of sensors and transducers. This device is the LED-photoresistor Mechanical-electrical Optoisolator Transducer.

The LED-photoresistor Mechanical-electrical Optoisolator Transducer combines the transducer feature to convert mechanical signals to electrical ones with the optoisolator feature of optical coupling between two voltage modules.

This is achieved by introducing a mechanically controlled system of Polaroid filters on the light beam path performing the optical coupling.

This sensor can be better miniaturized than optical sensors equipped with disk/disks with transparent and opaque areas.

Since the transducer output signal is an analog signal, it can be used to achieve simple circuits in automation, with a low cost price.

## 2. Experimental

### 2.1. Device principle and design

The Polaroid Optocoupler is a compound circuit optoelectronic device formed of: a light source, a photoreceiver, an assembly of two Polaroid filters (A-analyser and P-polariser) and a mechanical system (Fig.1), which can allow the axial fixation of these components as well as their setting in action [7], [8].

The mechanical system from Fig. 1 is made up of two identical mandrels (M), one for fixing the components of the polarizer-source system and the other one permitting the assembly of the analyser-receiver system's components.

Piece (1) is a socle for the light source, respectively the photoelectrical receiver, pieces (2), (3) allow the fixation of the polarizer and analyser filters, and piece (4), together with pieces (1), (2) and (3) form mount (M).

Pieces (5) allow mounts (M) to perform axial rotation movements, and the assembly made up of mount (M) and piece (4) can perform an axial translation movement within the guiding piece (6).

The light source of the LED-photoresistor Polaroid optocoupler is super bright white LED. Its bright intensity, on the direction of the longitudinal axis, is of  $(10365 \pm 226)$  mcd for a current of  $(19 \pm 0.01)$  mA.

As photoreceiver element we used a photoresistor type LDR07 [9].

The photoresistor supply voltage is  $V = (3 \pm 0.01)$  V.

Polaroid optocouplers can be designed in two forms: Polaroid optocouplers with and without distance adjustment.

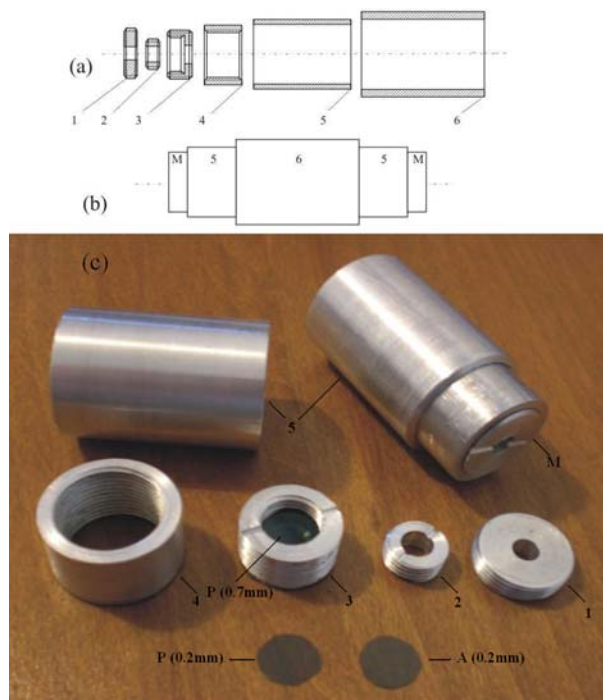


Fig. 1. The mechanical system of the Polaroid optocoupler.

In the case of Polaroid optocouplers without distance adjustment, misses piece (6) from figure (1) and piece (5) is common to both mounts (M).

In Fig. 2, are represented the circuit symbols of the LED-photoresistor Polaroid optocoupler in the two forms.

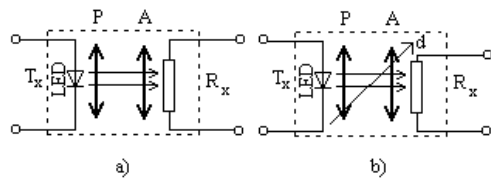


Fig. 2. LED-photoresistor Polaroid optocoupler: a) without distance adjustment, b) with distance adjustment.

LED-photoresistor Polaroid optocouplers without distance adjustment can be miniaturized by using the MEMS technology. For a good miniaturization it's preferred to replace the LED-Polaroid filter system with a polarized LED.

At the same time, this LED presents an increased energetic efficiency as compared to that one of the LED-Polaroid filter system [10], [11].

When the Polaroid optocoupler is used as mechanical-electrical transducer, the driver of the transmitter module ( $T_x$ ) is an independent current source.

In Fig. 3 is given the circuitry used to study the LED-photoresistor mechanical-electrical optoisolator transducer.

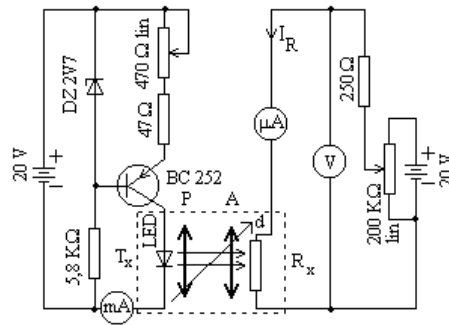


Fig. 3. Circuitry used in the study of the mechanical-electrical LED-photoresistor optoisolator transducer.

The driver of the module ( $T_x$ ) from this figure, maintains, through the LED, a constant current of 19 mA.

The intensity of the current through the LED is adjusted with the help of a linear potentiometer with a 470 Ohm resistance.

If the intensity of the current through the LED isn't modified in time, then, the intensity of the emitted light beam ( $J_0$ ) is constant.

This light beam performs the coupling between the transmitter module ( $T_x$ ) and the transducer's receiver module ( $R_x$ ).

The main characteristic of mechanical-electrical optoisolator transducers is to modify the intensity of the light beam which couples modules ( $T_x$ ) and ( $R_x$ ), as a result of two processes: one of polarization and the other one of re-orientation of the light beam's polarizing plan Fig. 4.

The intensity of the light beam being proportional with the square of the maximum value of the electrical field's intensity, according to Malus' law, one can write [12]:

$$J' = \frac{J_0}{2} \cdot \cos^2 \alpha, \quad (1)$$

where:

$J_0/2$  - the intensity of the light beam incident on the analyser filter;

$J'$  - the intensity of the light beam incident on the photoresistor's photosensible surface;

$\alpha$  - the angle between the polarization plans of the two Polaroid filters.

Equation (1) is true when the Polaroid filters are ideal, (the transmission, absorption and reflection coefficients in the vibration plan have the following values:  $T=1$ ,  $A=0$ ,  $R=0$  and, in any other plan, their values are:  $T'=0$ ,  $A'=1$ ,  $R'=0$ ).

According to (1), the relative rotation of the module ( $T_x$ ) towards module ( $R_x$ ), will determine the modification of the radiant flux incident on the receiver's surface.

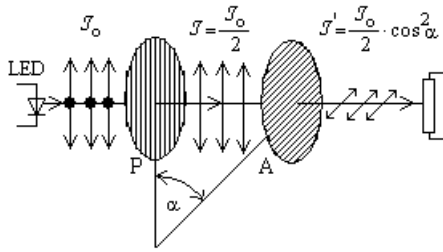


Fig. 4. Linear polarization and re-orientation of the light beam's polarizing plan, in a mechanical-electrical optoisolator transducer.

The value of the radiant flux incident on the receiver's surface also depends on distance (d) between the two modules.

In order to use this transducer in different applications, one must know its transfer function  $I_R=I_R(\alpha,d)$ .

2.2. Experimental characteristics

In order to study the dependence of the output current's intensity of the LED-photoresistor optoisolator transducer ( $I_R$ ) on angle( $\alpha$ ) and on the distance (d) between modules ( $T_x$ ) and ( $R_x$ ) there have been taken out the characteristics' families:  $I_R=I_R(\alpha)_{d=const}$  and  $I_R=I_R(d)_{\alpha=const}$ .

The experimental determinations were done for two sets of Polaroid filters. The widths of the Polaroid filters from the two sets are:  $h_1=0.2$  mm and  $h_2=0.7$ mm.

The values of the experimental determinations are presented in Table 1, ( $h_1=0.2$ mm) and Table 2, ( $h_2=0.2$ mm).

Table 1. Table with the intensities of the current through photoresistor expressed in ( $\mu A$ ), in the case of the set of filters  $h_1=0.2$  mm.

$\alpha$ (DE G)	d (mm)							
	78	83	88	93	98	103	108	113
0	435	384	346	310	279	255	232	213
10	425	375	340	300	270	250	230	205
20	400	360	325	285	260	240	215	195
30	365	325	300	260	240	220	200	175
40	325	285	255	230	215	195	175	153
50	270	240	215	200	180	165	150	125
60	220	195	175	165	140	132	116	100
70	170	150	135	125	105	100	88	75
80	125	110	96	90	80	75	70	56
90	98	87	78	70	63.5	57.5	52.5	48

By graphically representing the data from Table 1 and Table 2 are obtained the characteristics' families:  $I_R=I_R(\alpha)_{d=const}$  and  $I_R=I_R(d)_{\alpha=const}$  in the case of the two sets of filters, Fig. 5, Fig 6, Fig.7, Fig. 8.

Table 2. Table with the intensities of the electrical current through photoresistor expressed in ( $\mu A$ ), in the case of the set of filters  $h_2=0.7$  mm.

$\alpha$ (DE G)	d (mm)							
	78	83	88	93	98	103	108	113
0	105	95	87	78	71	65	60	56
10	102	93	84	75	70	64	59	54
20	95	85	77	70	65	58	54	50
30	85	75	67	60	56	51	47	44
40	70	63	55	51	46	42	39	37
50	54	47	43	40	36	33	31	29
60	35	32	30	27	25	23	21	19
70	22	19	18	17	15	14	12	12
80	12	10	10	9	8	7	7	6
90	7.2	6.5	5.9	5.3	4.9	4.5	4.1	3.8

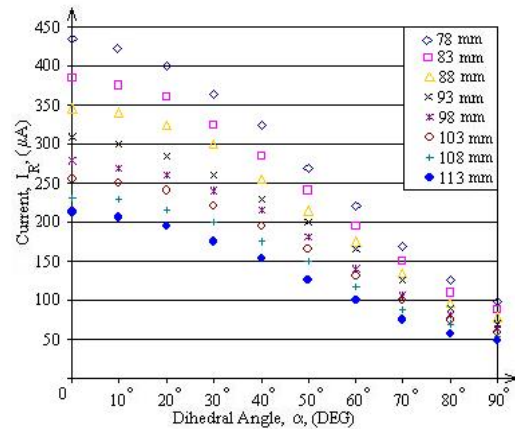


Fig. 5. The transfer characteristics family  $I_R=I_R(\alpha)_{d=const}$  of the LED-photoresistor mechanical-electrical optoisolator transducers, ( $h_1=0.2$  mm).

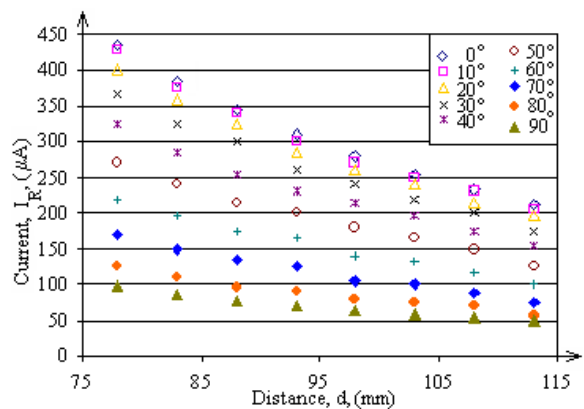


Fig. 6. The transfer characteristics family  $I_R=I_R(d)_{\alpha=const}$  of the LED-photoresistor mechanical-electrical optoisolator transducers, ( $h_1=0.2$  mm).

**2.2. Characteristics modelling**

In the case of photoresistors, the dependence of the illumination photocurrent ( $I_L$ ), is caused by the dependence of photoconductivity ( $\Delta\sigma$ ) on illumination.

$$I_L \sim \Delta\sigma \tag{2}$$

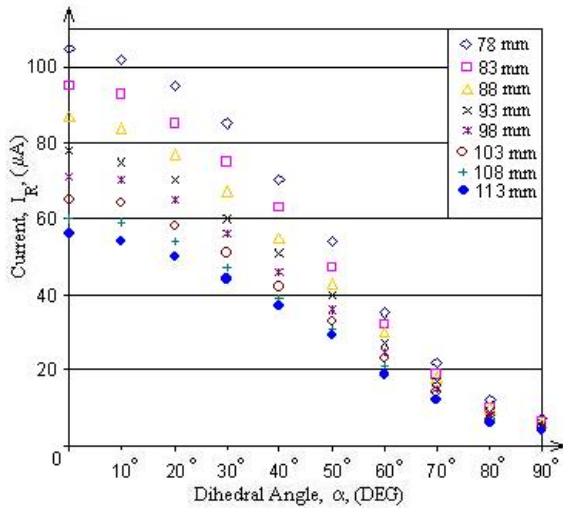


Fig. 7. The transfer characteristics family  $I_R=I_R(\alpha)_{d=const.}$  of the LED-photoresistor mechanical-electrical optoisolator transducers, ( $h_2=0.7$  mm).

In stationary regime, in the case of generating and recombining exclusively bend-to-bend and particularized for small widths of the sample, the intensity of the photocurrent ( $I_L$ ) depends on the radiant illumination ( $E_c$ ) by a relation like:

$$I_L = C \cdot E_c^a \cdot V \tag{3}$$

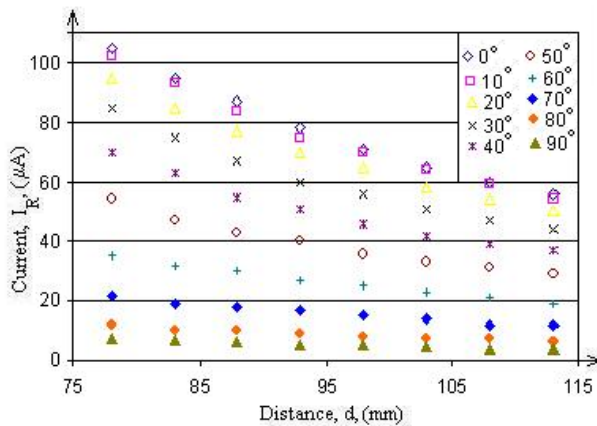


Fig. 8. The transfer characteristics family  $I_R=I_R(d)_{\alpha=const.}$  of the LED-photoresistor mechanical-electrical optoisolator transducers, ( $h_2=0.7$  mm).

Since between the radiant and the luminous illumination ( $E_v$ ), there is a relation of direct proportionality, expression (3) can be written as:

$$I_L = C \cdot k(\lambda) \cdot E_v^a \cdot V = C_1 \cdot E_v^a \cdot V \tag{4}$$

where:

$$C_1 = C \cdot k(\lambda) \tag{5}$$

The constants intervening in (4) and (5) have the following significances:

- $C$  – is a proportionality constant specific to the photoresistor. It doesn't depend on the illumination and on the voltage ( $V$ ) applied to the photoresistor.
- $k(\lambda)$  – represents the luminous spectral efficacy of the optical radiation (radiation photometrical equivalent);
- $a$  – is a parameter depending on the level of the photoresistor's illumination.

In the case of photoresistor LDR07, the intensity of the dark current ( $I_d$ ) is negligible as compared to the intensity of photocurrent ( $I_L$ ).

$$I_R = I_L + I_d \approx I_L \tag{6}$$

If the supply voltage of LDR07 photoresistor is constant, from (4) and (6) there results:

$$I_R = C_2 \cdot E_v^a \tag{7}$$

where, constant  $C_2 = V \cdot C_1$ .

In the case of punctiform light sources, when the light beam normally falls on the photoresistor's photosensible surface, the relation below is true:

$$E_v = \frac{I_v}{d^2} \tag{8}$$

where:

- $I_v$  – the radiation's luminous intensity;
- $d$  – the distance from the light source up to the p

In practice, this relation can be used if the "rule of the ten diameters is respected", (the detector's diameter must be ten times smaller than distance ( $d$ )).

Measurement errors obtained in this case are smaller than 1 %.

Knowing that both the intensity of the light beam falling on the photoresistor's surface and its luminous illumination are proportional with the square of the maximum value of the electrical field's intensity, from relations (1) and (8) results:

$$E_v = \frac{C_3 \cdot \mathcal{J}'}{d^2} = \frac{C_3 \cdot \frac{\mathcal{J}_0}{2} \cdot \cos^2 \alpha}{d^2} = \frac{C_4 \cdot \cos^2 \alpha}{d^2} \tag{9}$$

where:  $C_4 = C_3 \cdot \frac{\mathcal{J}_0}{2}$

From (7) and (9) results:

$$I_R = C_2 \cdot \left( \frac{C_4 \cdot \cos^2 \alpha}{d^2} \right)^a \quad (10)$$

Expression (10) is a function showing the dependence of the current's intensity through photoresistor on the dihedral angle ( $\alpha$ ) and on the distance ( $d$ ) between ( $T_x$ ) and ( $R_x$ ) modules.

From (10) can be observed that, for  $\alpha=90^\circ$ , the intensity of the optocoupler's output current is equal with zero. In practice, this thing isn't possible, since the Polaroid filters aren't ideal. Although in the filter's polarizing plan, at its output, the light flux should be null, in reality, there is an emergent light flux different from zero, (Figures 5, 6, 7, 8).

In this case (10) becomes:

$$I_R = C_2 \cdot C_4^a \cdot \frac{(\cos^{2a} \alpha + T)}{d^{2a}} \quad (11)$$

where ( $T$ ) represents the fraction from the intensity of the light beam falling on the analyser filter and succeeding in passing through it, in case of extinction.

In the case when the distance between modules ( $T_x$ ) and ( $R_x$ ) is constant, (11) can be written as:

$$I_R = C_5 \cdot (\cos^{2a} \alpha + T) \quad (12)$$

where  $C_5$  is a constant.

Expression (12) is a function in the form of  $I_R = I_R(\alpha)$ .

In order to graphically represent (12) on the interval  $0^\circ \leq \alpha \leq 90^\circ$ , one must determine the extreme and the inflexion points of the function.

Equation (13) represents the first-order derivative of function (12).

$$I_R' = -C_5 \cdot 2a \cdot \sin \alpha \cdot \cos^{2a-1} \alpha \quad (13)$$

A solution of the equation  $I'(\alpha) = 0$ , on the studied interval is  $\alpha_1 = 0^\circ$ .

Equation (14) represents the second-order derivative of function (12).

$$I_R'' = -C_5 \cdot 2a \cdot [\cos^{2a} \alpha - (2a-1) \cdot \sin^2 \alpha \cdot \cos^{2a-2} \alpha] \quad (14)$$

$$I_R''(0^\circ) = -2aC_5 < 0 \quad (15)$$

From (15) can be noticed that in point ( $\alpha_1=0^\circ$ ), function  $I_R = I_R(\alpha)$ , presents a maximum.

If parameter  $a > 0.5$ , on the studied interval, equation  $I_R'(\alpha) = 0$  also presents a solution,  $\alpha_2 = 90^\circ$ .

The superior-order derivatives of function (12) can be written in the form:

$$I^{(n)} = A(a, \alpha) \pm B(a) \cdot \sin^n \alpha \cdot \cos^{2a-n} \alpha \quad (16)$$

where:

- function  $A=A(a, \alpha)$ , is reduced to zero in the point  $\alpha_2 = 90^\circ$ ;

-  $B(a) > 0$ ;

- the sign „+” appears when the derivative's order ( $n$ ) is an even number and the sign „-” appears in the case when the derivative's order ( $n$ ) is an odd number.

According to the value of the parameter ( $a$ ), are calculated the superior-order derivatives of function  $I=I(\alpha)$  in the point  $\alpha_2 = 90^\circ$  until is found a derivative different from zero,  $I_R^{(n)}(90^\circ) \neq 0$ .

If the order of this derivative is an even number, the function will present a minimum in the point  $\alpha_2=90^\circ$ . If the order of this derivative class is an odd number, then, that point is an inflexion point for function  $I_R=I_R(\alpha)$ . On a small interval around this point, the graphic can be considered to be parallel with the abscissa.

From equation  $I_R''(\alpha)=0$  is obtained the value of angle „ $\alpha_1$ ”, for which the function presents an inflexion point in the interval  $0^\circ \leq \alpha \leq 90^\circ$ , relation (17).

$$\operatorname{tg} \alpha_1 = \frac{1}{\sqrt{2a-1}} \quad (17)$$

From (17) results that function  $I_R = I_R(\alpha)$  presents an inflexion point in the domain  $0^\circ \leq \alpha \leq 90^\circ$ , only if  $a > 0.5$ .

From Fig. 5 and Fig. 7, can be noticed that, in the case of our transducer  $a > 0.5$ .

In this case, (11) presents two extreme points: a maximum for  $\alpha_1 = 0^\circ$  and minimum for  $\alpha_2 = 90^\circ$ .

- from (15) can be noticed that, in case of extinction ( $\alpha_2=90^\circ$ ), the intensity of the optocoupler's output current isn't equal with zero.

If the distance between modules ( $T_x$ ) and ( $R_x$ ) is modified, and the angle ( $\alpha$ ) is maintained constant, (11) can be written in the form:

$$I_R = \frac{C_4^a \cdot C_6}{d^{2a}} \quad (18)$$

From relation (18) can be noticed that function  $I_R=I_R(d)_{\alpha=\text{const}}$  doesn't present extreme or inflexion points. If  $d \rightarrow \infty$ ,  $I_R \rightarrow 0$  and if  $d \rightarrow 0$ ,  $I_R \rightarrow \infty$ .

In order to graphically represent function (11) one must determine the constants' values.

Writing (11) in particular cases  $\alpha=0^\circ$  and  $\alpha=90^\circ$ , results:

$$I_{R0^\circ} = C_2 \cdot C_4^a \cdot \frac{(1+T)}{d^{2a}} \quad (19)$$

$$I_{R90^\circ} = C_2 \cdot C_4^a \cdot \frac{T}{d^{2a}} \quad (20)$$

From (19) and (20) is obtained the expression of the transmission coefficient ( $T$ ).

$$T = \frac{I_{R90^\circ}}{I_{R0^\circ} - I_{R90^\circ}} \quad (21)$$

The transmission coefficient has been calculated for each one of the family's characteristic  $I_R=I_R(\alpha)_{d=\text{const}}$ . This

coefficient's average values for the two sets of filters are:  $T_1=0.292$  for  $h_1=0.2$  mm and  $T_2=0.073$  for  $h_2=0.7$  mm. From (11) for  $\alpha=90^\circ$ , is obtained:

$$C_5 = C_2 \cdot C_4^a = \frac{I_{R90^\circ} \cdot d^{2a}}{T} \quad (22)$$

In this case (11) becomes:

$$I_R = \frac{I_{R90^\circ} \cdot d^{2a}}{T} \cdot (\cos^{2a} \alpha + T) \quad (23)$$

Constants (a) and ( $C_5$ ) are determined by superposing the characteristics given by (23) over the experimental characteristics from Fig. 7.

In the case of low illuminations ( $h_2=0.7$ mm), for all the family's characteristics, for  $I_R=I_R(\alpha)_{d=const.}$ ,  $a=0.87$ . The values of constant ( $C_5$ ) being very close among them, in (11) can be used the medium value of this constant  $C_{5m}=193.44 \text{ mA} \cdot (\text{mm})^{2a}$ .

In this case, (11) becomes:

$$I_R = 193.44 \text{ mA} \cdot (\text{mm})^{1.74} \cdot \frac{(\cos^{1.74} \alpha + 0.073)}{d^{1.74}} \quad (24)$$

At more intense illuminations, the case of filters ( $h_1=0.2$ mm), the dependence of parameter (a) on illumination can't be neglected at all.

Using (23) and the characteristics from Fig. 5, one can determine the values of constants (a) and ( $C_5$ ) for each characteristic.

The values of constant ( $C_5$ ) being very close among them, one works with the arithmetical mean of these ones  $C_{5m}=151.29 \text{ mA} \cdot (\text{mm})^{2a}$ .

The dependence of constant (a) on distance (d) is represented in Fig. 9, curve a).

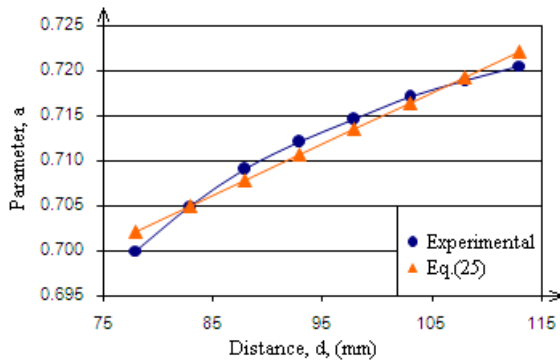


Fig. 9. a) The dependence of parameters (a), experimentally determined, on distance (d); b) The representation of the empirical function (25).

Using the method of least squares, on the basis of the graphic from Fig. 9.a) was obtained the empirical function

$a=a(d)$ . It represents the dependence of parameter (a) on distance (d), (25).

$$a \cong 0.66 + 5.7 \cdot 10^{-4} \text{ mm}^{-1} \cdot d \quad (25)$$

In the case of using filters ( $h_1=0.2$ mm), (11) becomes:

$$I_R = 151.29 \text{ mA} \cdot (\text{mm})^{2a} \cdot \frac{[\cos^{2 \cdot (0.66 + 5.7 \cdot 10^{-4} \text{ mm}^{-1} \cdot d)} \alpha + 0.292]}{d^{2 \cdot (0.66 + 5.7 \cdot 10^{-4} \text{ mm}^{-1} \cdot d)}} \quad (26)$$

### 3. Results and discussion

In Fig. 10 and Fig. 11 are rendered the two-dimensional graphic representations  $I_R=I_R(\alpha)_{d=const.}$  and  $I_R=I_R(d)_{\alpha=const.}$  of equation (24).

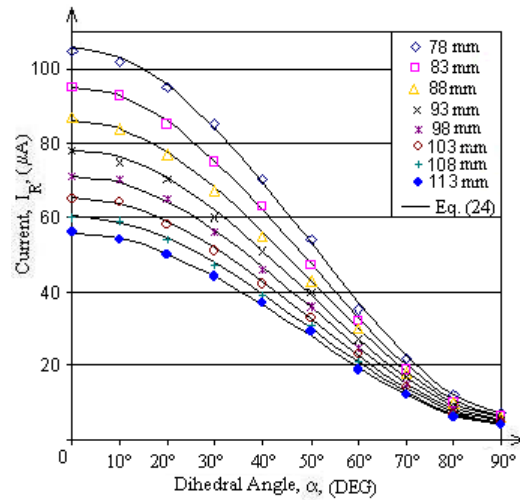


Fig. 10. The families of the theoretical and experimental characteristics  $I_R=I_R(\alpha)_{d=const.}$  of the optoisolator transducer, in case of filters ( $h_2=0.7$ mm)

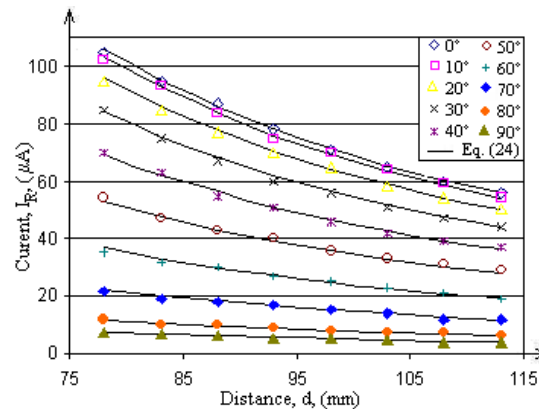


Fig. 11. The families of the theoretical and experimental characteristics  $I_R=I_R(d)_{\alpha=const.}$  of the optoisolator transducer, in case of filters ( $h_2=0.7$ mm)

For comparison with the experimental data, in these graphics are also represented the points corresponding to the characteristics' family  $I_R=I_R(\alpha)_{d=const.}$  and  $I_R=I_R(d)_{\alpha=const.}$  from Fig. 7 and Fig. 8.

From these figures, can be noticed that at low illuminations ( $h_2=0.7mm$ ), the dependence of parameter (a) on illumination is negligible.

In Fig. 12 is rendered the (3-D) graphical representation  $I_R=I_R(\alpha, d)$ , of equation (24).

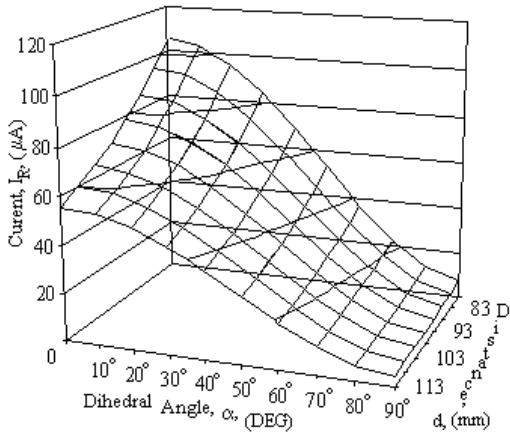


Fig. 12. The 3D representation of the theoretical characteristics' family  $I_R=I_R(\alpha, d)$ , in case of filters ( $h_2=0.7mm$ )

In Fig. 13 and Fig. 14 are rendered the two-dimensional representations of function (26). These representations are superposed over the points corresponding to the characteristics' family  $I_R=I_R(\alpha)_{d=const.}$  and  $I_R=I_R(d)_{\alpha=const.}$  from Fig. 5 and Fig. 6.

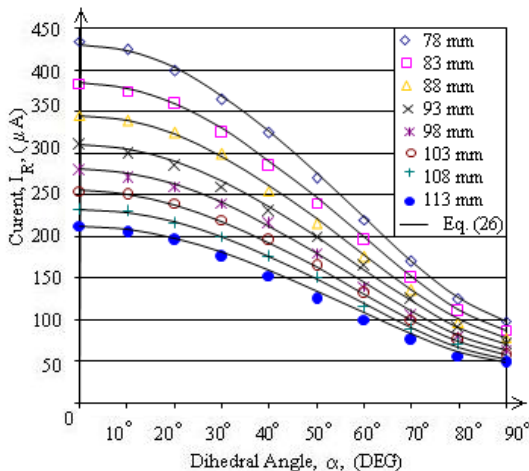


Fig. 13. The families of the theoretical (Eq. 26) and experimental characteristics  $I_R=I_R(\alpha)_{d=const.}$ , of the optoisolator transducer, in case of filters ( $h_1=0.2mm$ )

This time, the dependence of parameter (a) on illumination can't be neglected at all.

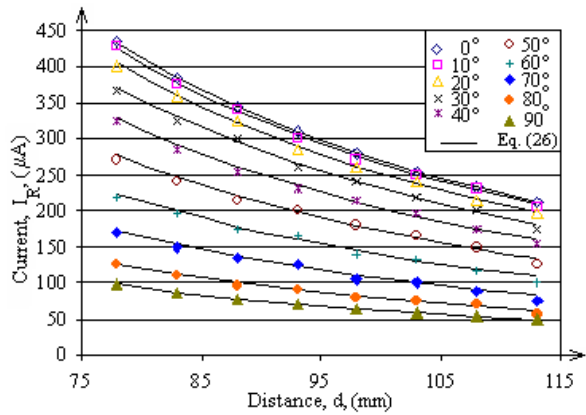


Fig. 14. The families of the theoretical (Eq. 26) and experimental characteristics  $I_R=I_R(d)_{\alpha=const.}$ , of the optoisolator transducer, in case of filters ( $h_2=0.2mm$ )

The effect of neglect, at more intense illuminations, of the dependence of parameter (a) on illumination, can be observed in Fig. 15 and Fig. 16.

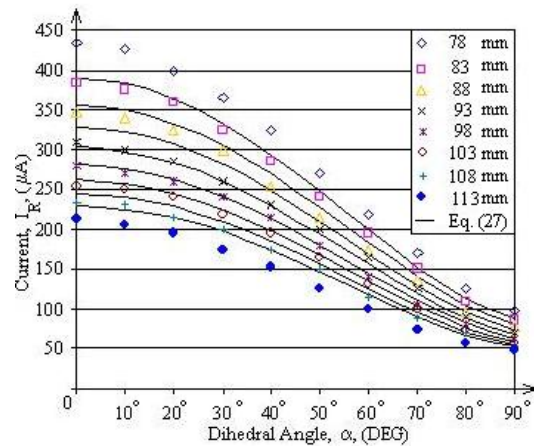


Fig. 15. The families of the theoretical (Eq. 27) and experimental characteristics  $I_R=I_R(\alpha)_{d=const.}$ , of the optoisolator transducer, in case of filters ( $h_1=0.2mm$ )

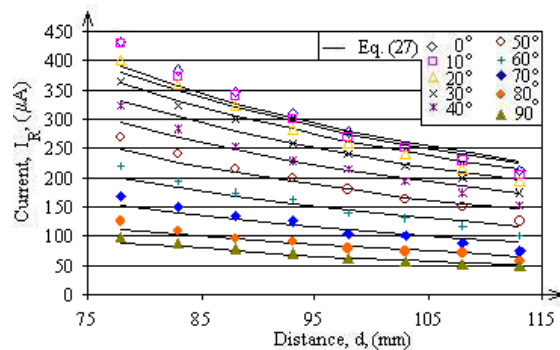


Fig. 16. The families of the theoretical (Eq. 27) and experimental characteristics  $I_R=I_R(d)_{\alpha=const.}$ , of the optoisolator transducer, in case of filters ( $h_1=0.2mm$ ).

In these representations, instead of function (25) we used the arithmetical mean of parameters (a), ( $a_m=0.7121$ ). In this case (26) becomes:

$$I_R = 151.29\text{mA} \cdot (\text{mm})^{2a} \cdot \frac{(\cos^{1.4242} \alpha + 0.292)}{d^{1.4242}} \quad (27)$$

If in case of more intense illuminations is used parameter ( $a_m$ ), (27) will describe very well the behavior of the transducer, only for medium values of distance (d). The theoretical characteristics corresponding to the extreme values of distance (d) will approach to the central area of the characteristics' family  $I_R=I_R(\alpha)_{d=\text{const.}}$ , Fig. 15.

The neglect of the dependence of parameter (a) on illumination, in Fig. 16 has, as effect, a slight rotation to the left of the characteristics  $I_R=I_R(d)_{\alpha=\text{const.}}$ , towards their central area.

While analysing the phenomena taking place during the process of converting the rotation/translation movements into electrical current, we haven't talked about light's absorption and reflection processes, which occur in the area of polaroid filters. Practically, the effects of absorption and reflection coefficients are comprised in constant ( $C_2$ ) from (11).

If in (11) we explicitly introduce these coefficients, it will be in the form below:

$$I_R = C_2' \cdot (1 - A - R) \cdot C_4^a \cdot \frac{(\cos^{2a} \alpha + T)}{d^{2a}} \quad (28)$$

#### 4. Conclusions

LED-photoresistor mechanical-electrical optoisolator transducers turn rotation and/or translation movements into electrical signals. They can simultaneously provide a processor with information related to: the position, the – movement direction, the speed and the acceleration of a component of a mechanical device.

If the Polaroid optocoupler is to be part of complex systems, the command can be performed both by rotation movements (modification of angle  $\alpha$ ) and by translation movements (modification of distance  $d$ ).

Modification of distance (d) can be also used to compensate the effects caused by the ageing of the LED.

It is preferred that the employed filters couldn't allow a too big illumination of the photoresistor. In this case, parameter (a) is practically constant.

When the signal provided by the transducer must have a bigger value, one must use an empirical relation in the type of  $a=a(d)$ .

If the employed transducer isn't fitted with distance adjustment, parameter (a) can be considered constant.

As compared to mechanical-electrical transducers which use one or two disks fitted with clefts, these transducers can be miniaturized. At the same time, the replacement of the cleft disk(s) with the system of Polaroid filters, allows the continuous determination of

movement parameters of the mechanical system's component.

Optoisolator transducers can be connected to the IEEE 1451.4 standard interface.

Mechanical-electrical optoisolator transducers are mainly designed to be applied in the field of mechatronics.

#### Acknowledgment

This work was partially supported by European Framework Program 7 under the contract no. PIRG02-GA-2007-224904.

#### References

- [1] V. Sridhar, K. Takahata, *Sensors and Actuators A: Physical*, **155** (1), 58 (2009).
- [2] A. Dybko, J. Zachara, J. Golimowski, W. Wróblewski, *Analytica Chimica Acta*, **485** (1), 103 (2003).
- [3] S. Jia, G. Ding, X. Zhao, C. Yang, *Optics & Laser Technology*, **39** (2), 353 (2007).
- [4] M. Kraft, A. Kenda, T. Sandner, H. Schenk, MEMS-based compact FT-spectrometers - a platform for spectroscopic mid-infrared sensors, *Proc. IEEE Intern. Conf. Sensors*, 130 (2008).
- [5] A.T. Gambutan, M. Popa, Smart homes. A solution for a smart lighting system, *Proc. IEEE 5-th Intern. Symp. on Applied Computational Intelligence and Informatics*, 205 (2009).
- [6] M. Pahlang, E. Zahedi, M.A.B.M. Ali, *Proc. IEEE EMBS Asian-Pacific Conference on Biomedical Engineering*, 322 (2003).
- [7] I. M. Ciuruş, Optocuplor polaroid, (patent pending) OSIM Bucureşti, a2009 00270, (2009).
- [8] I.M. Ciuruş, M. Dimian, A. Graur, *Optoelectronics and Advanced Materials-Rapid Communications*, **4** (9), 1366 (2010).
- [9] <http://www.datasheetarchive.com/LDR07-datasheet.html#>.
- [10] J. Wheatley, C. Leatherdale, A. Ouderkirk, *Polarized LED*, PCT/US2005/034300
- [11] M.F. Schubert, S. Chhajed, J.K. Kim, E.F. Schubert, J. Cho, *Optics Express*, **15**(18), 11213 (2007).
- [12] I.M. Ciuruş, M. Dimian, A. Graur, *Proc. IEEE 12<sup>th</sup> Intern. Conf. Optimization of Electrical and Electronic Equipment*, 740 (2010).

\*Corresponding author: marcelciurus@usv.ro